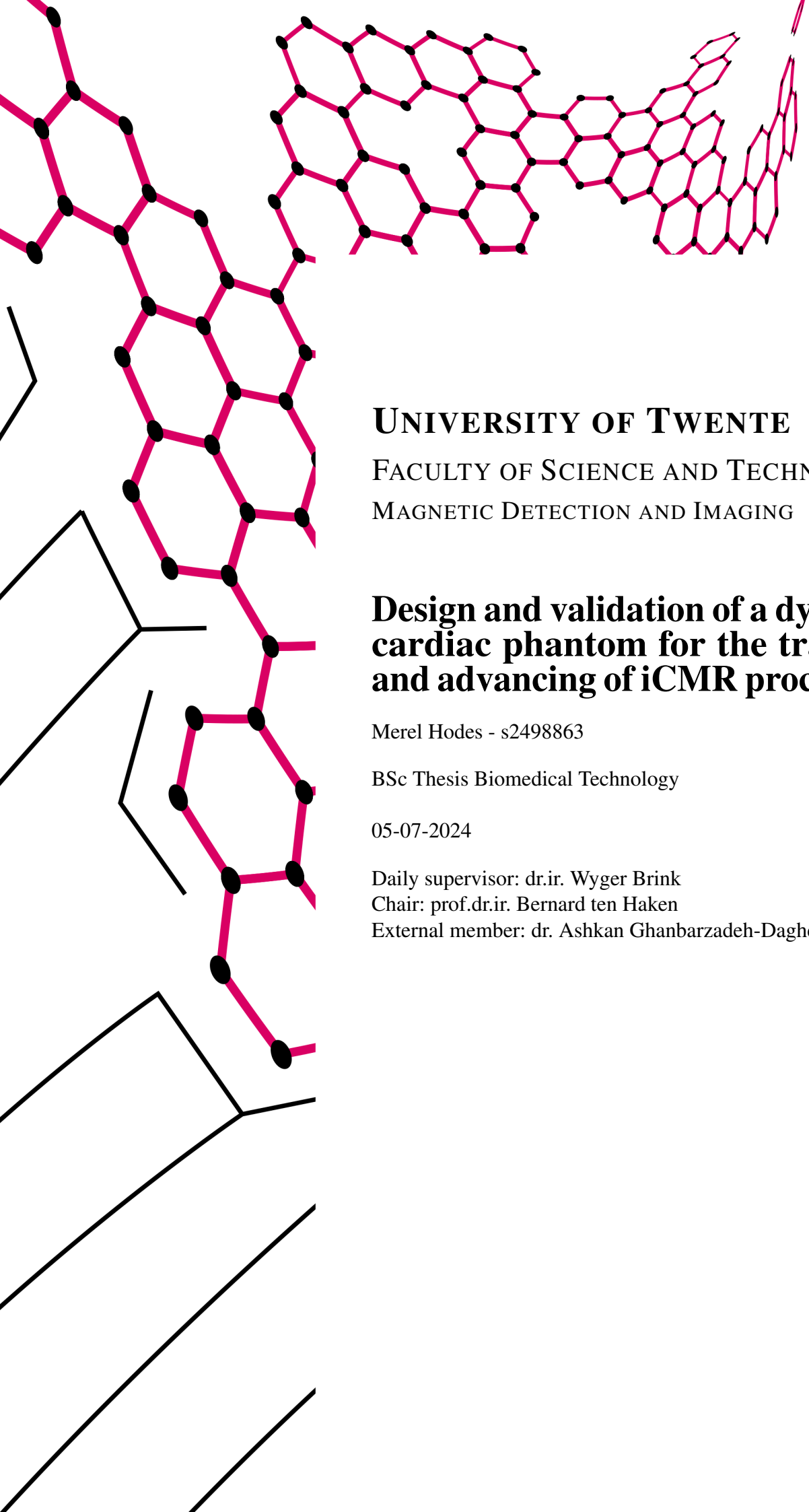

UNIVERSITY OF TWENTE

FACULTY OF SCIENCE AND TECHNOLOGY

MAGNETIC DETECTION AND IMAGING

Design and validation of a dynamic cardiac phantom for the training and advancing of iCMR procedures

Merel Hodes - s2498863

BSc Thesis Biomedical Technology

05-07-2024

Daily supervisor: dr.ir. Wyger Brink
Chair: prof.dr.ir. Bernard ten Haken
External member: dr. Ashkan Ghanbarzadeh-Dagheyan

Abstract

Cardiovascular diseases (CVDs) remain the leading cause of death worldwide. When treating these diseases, a minimally invasive approach is favored. Interventional cardiac magnetic resonance (iCMR) procedures are particularly useful in these situations. These catheter based procedures offer a less invasive alternative to traditional methods. However, since these techniques are still relatively new, there is a substantial need for further development and training. This paper looks at the design, fabrication and validation of a dynamic cardiac phantom constructed from silicone, intended for the training and development of these iCMR procedures. The iterative design process revolved around mold optimization, with its main focus on correct centering. The acquired phantom was subjected to multiple assessments to evaluate its dynamic capabilities, structural integrity and suitability for iCMR training. Tests were done using a pressure vessel forcing the phantom to contract due to an increase and decrease in external pressure. MRI-based testing confirmed its functionality, showing contraction and effective catheter tracking. Pressure testing showed the phantom's ability to remain intact at normal heart pressures. In conclusion, the research confirms the feasibility of using silicone to create a dynamic cardiac phantom for the development and training of iCMR procedures.

Contents

1 Introduction

Cardiovascular diseases (CVDs) are the leading cause of death worldwide, taking approximately 17,9 million lives each year. [1] In the Netherlands 22,9% of all deaths are caused by these diseases. [2] The most prevalent conditions within CVDs are atrial fibrillation and valve diseases.

1.1 iCMR

Minimally invasive approaches are favored in the treatment of CVDs. These approaches reduce damage to the body, speed up the healing process and minimize complications. However, clinicians heavily rely on good visualization of the anatomy and hand eye coordination during such procedures. Cardiovascular magnetic resonance (CMR) is an imaging technique used for visualizing the heart. With the use of MRI technology, CMR provides a number of advantages over more conventional techniques like CT, ultrasound or X-ray. It eliminates radiation, has unconstrained imaging planes and offers high quality image contrast. [3] Interventional cardiovascular magnetic resonance (iCMR) refers to therapeutic catheter-based procedures using CMR for guidance instead of the more conventional radiographic guidance. [4] Examples of these procedures are radio-frequency ablation and diagnostic cardiac catherization. [5] These procedures are less invasive due to the use of catheters and CMR guidance, which allows for a clear view of the patients heart without having to open up their chest. Another benefit of using CMR instead of radiographic guidance is the lack of radiation exposure to both the patient and the clinical staff. [4] Furthermore CMR enables "real-time" imaging, providing clinicians direct visualization of the cardiac anatomy during the procedure.

In vivo porcine and bovine hearts are commonly utilized for training and developing cardiac procedures. [6] This choice is due to the anatomical similarities between these animal hearts and the human heart. Making use of porcine and bovine hearts allows for simulation of the human cardiovascular system and assessment of the bio-compatibility of certain appliances used during these procedures. Moreover, practicing procedures on a beating heart introduces additional complexities, allowing clinicians to acquire essential skills necessary before actually operating on human patients. However, access to these animals is constrained due to limited availability, making them fairly expensive. In addition, using an alive animal to train these procedures raises certain ethical concerns. Therefore, other alternatives are needed to facilitate training and developing minimally invasive cardiac procedures. A possible solution to this problem would be to create a dynamic cardiac phantom made out of silicone, that is visible on MRI. There are several advantages to using a silicone cardiac phantom. As mentioned before, it is less expensive and more ethical compared to biological alternatives. Additionally, silicone phantoms are reusable, as they do not biologically deteriorate over time, are more hygienic to work with and provide precise control over shape and size, enabling the creation of patient-specific models. The phantom must mimic the properties and characteristics of the heart and facilitate the training and development of interventional cardiac procedures like radio-frequency ablation and diagnostic cardiac catheterization. In addition the phantom must be dynamic to replicate the settings of a beating heart.

1.2 Anatomy and physiology of the heart

To create a phantom that simulates the heart, knowledge of its anatomy and physiology is essential.

The heart is composed of two atria and two ventricles. Deoxygenated blood initially enters the right atrium through the vena cava where it passes via the tricuspid valve into the right ventricle. [7] From there it is pushed through the pulmonary artery towards the lungs for oxygenation. The pulmonary veins then carry the oxygen-rich blood back to the heart where it enters the left atrium and passes through the mitral valve to reach the left ventricle. Finally the left ventricle pushes the oxygenated blood through the aorta, distributing it throughout the body where the oxygen can be absorbed by different parts of the body. Each chamber of the heart undergoes distinct phases of volume and pressure. This relation can be depicted in pressure volume loops as seen in figure 2. These pressure volume loops are determined by using catheters to measure the pressure in a certain part of the heart. Simultaneously the ventricular volume can be evaluated using magnetic resonance imaging (MRI). [8] Validating the heart's function can be achieved by building a phantom that is capable of producing these pressure volume loops.

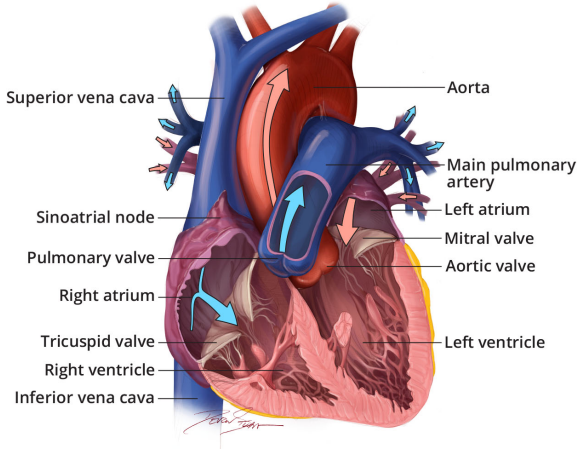

Figure 1: Anatomy of the interior of the heart. [7]

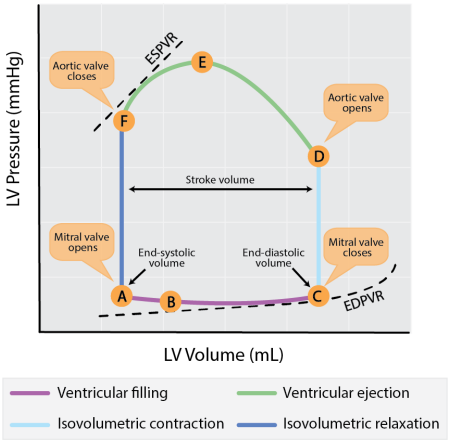

Figure 2: Pressure volume loop including different phases during a cardiac cycle. [9]

1.3 Silicone

Silicone is a widely used material for organ phantoms. It has been used for the creation of breast phantoms and for mimicking lung tissue, skin, muscle and fat. [10] [11] The elasticity of the material allows for the creation of dynamic models. Consequently, silicone offers a solid foundation for the development of a cardiac phantom. [12] The mechanical properties of silicone can be easily altered by changing the amount of cross-linking. A low amount of cross-linking will result in very flexible silicones with a low Youngs modulus. As seen in figure 3 silicones with a low Youngs modulus will be good for mimicking cerebral tissue or skin tissue. A higher amount of cross-linking will result in a higher Youngs modulus which will be favorable when mimicking cartilage or tendons.

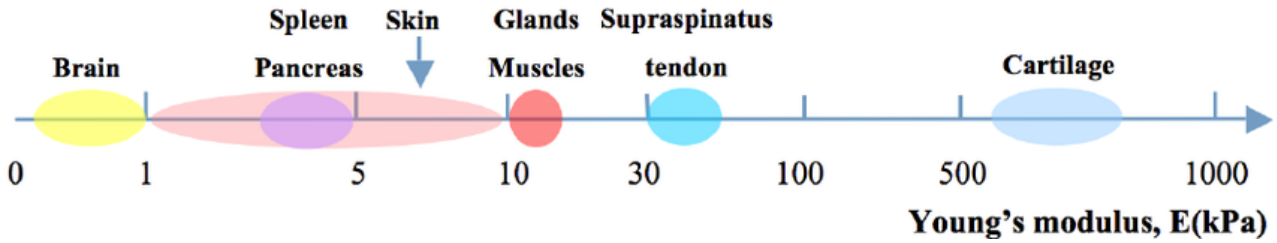

Figure 3: Different tissues and their Youngs modulus. [13]

The current inability of silicone to be 3D printed is a major factor in the lack of silicone cardiac phantoms. As a result it needs to be poured into a mold. However silicone is an excellent material for making intrinsic phantoms due to its low viscosity prior to curing and high resistance to fractures following curing. Complete filling of the mold will be possible since the fluid silicone can get into all crevices and corners. One of the largest obstacles when pouring silicone is the formation of air bubbles. To prevent this formation, the fluid silicone can be degassed under vacuum. Another benefit to silicone is that it is MR compatible. The T1 relaxation time of silicone closely resembles the T1 relaxation time of adipose tissue which makes it a preferred choice in phantom design for MRI since this similarity ensures that silicone is clearly visible in images. [14]

1.4 State of the art

Currently, several studies have focused on the design and fabrication of dynamic cardiac phantoms. Liang et al. did a study were a patient specific cardiac phantom was developed to simulate a MitraClip® procedure. [15] In this study both silicone and PVA-c were used as tissue mimicking materials. A flexible silicone outer mold and a rigid inner mold, representing the blood pool, were used. This rigid inner mold resulted in the limitation that the entire bottom of the phantom was flat and thus not anatomically correct. Moreover, the phantom in this research was not subjected to any additional pressure. Consequently, there had been no testing to evaluate training the procedures in dynamic conditions, such as those presented by a beating heart.

A different research performed by Kolawole et al. created cardiac phantoms to validate MRI-derived myocardial stiffness estimates. [16] In this study, a rigid outer mold, made of polylactic acid (PLA) and a rigid inner mold, made of water soluble polyvinyl alcohol (PVA), were used. Silicone's of different stiffness's were used and poured into the mold. After curing, the inner mold could be dissolved using water, and a silicone cardiac phantom would remain. In this study, similar to the study of Laing et al., the bottom of the phantom was flat resulting in a left ventricle that would not simulate the heart properly.

A third paper by Bietenbeck et al. produced a CMR-conditional cardiac phantom simulating cardiac anatomy and function and which enabled training of iCMR procedures. [17] The phantom in this research was composed of MR-safe or -conditional materials. The phantom comprised two atrial and two ventricular chambers that were linked via four cardiac valves. Though this is similar to the human heart, the chambers and the phantom itself were not anatomically correct. They were able to realize

systolic contraction by increasing external pressure. The external pressure caused movement of the elastic membrane of the ventricle wall, resulting fluid to be pressured into the chambers next to the ventricles. Diastolic relaxation was realized by decreasing the external pressure.

A final research by Cohrs et al. produced a soft total artificial heart. [18] The aim of this study was to present an innovative concept of a soft artificial heart. This heart was made out of silicone and poured into a poly(acrylonitrile-co-butadiene-co-styrene)-plastic (ABS) mold which, after curing, could be dissolved in a acetone bath. This model came very close to being anatomically correct. However, the model had a limited durability and broke after about 3000 beats.

1.5 Aim

The aim of this paper is the development of a dynamic cardiac phantom for the purpose of training and advancing minimally invasive iCMR procedures. A design approach is considered to fabricate an anatomically correct cardiac phantom using silicone. The goal is to validate the obtained phantom by creating pressure curves and dynamic imaging using MRI techniques.

This leads to the following research question:

"What is the feasibility of using silicone to create a dynamic cardiac phantom that would be used for the training and development of iCMR procedures?"

2 Requirements

A list of requirement is drafted based on the conducted background research and discussion with experts. This list serves as a guideline in the creation and assessment of the final design. The requirements were ranked using the MoSCoW method. [19] According to this method all requirements were systematically grouped into four categories: Must have, Should have, Could have and Won't have.

Table 1: List of requirements

	Requirements	*MoSCoW*
1	**Cardiac Phantom**	
1.1	The phantom is made out of silicone	M
1.2	The phantom has a Youngs modulus comparable to the myocard	C
1.3	The atria and ventricles of the phantom are anatomically correct	S
1.4	The phantom is MR compatible	M
1.5	The blood pool is not included in the phantom	M
1.6	The phantom contains valves	W
2	**Function**	
2.1	The phantom is dynamic	M
2.2	The phantom stays intact at normal heart pressure	M
2.3	The phantom allows for pressure curves to be created	M
2.4	The phantom allows for the training of iCMR procedures	M

2.1 Cardiac phantom

This set of requirements is related to the material and appearance of the cardiac phantom. Firstly, since silicone is a material that is well suited for creating a cardiac phantom, as was discussed in the preceding section, the phantom must be made out of silicone. This silicone could have a Youngs modules that compares to the Youngs modulus of the myocard, creating a similar elasticity to the cardiac tissue. Furthermore the model should be as anatomically correct as possible, prioritising the atria and ventricles. The atria and ventricles are included by removing the blood-pool from the phantom. Lastly the phantom must be MR compatible to enable use within the MRI environment.

2.2 Function

The second set of requirements involves the function of the cardiac phantom. First of all the phantom must be dynamic, mimicking the movement of the heart. Secondly, the phantom must stay intact at at least 120-150 mm Hg, as this is a average peak pressure in the left ventricle. [20] Additionally, the phantom must allow for pressure curves to be created as this serves as validation of the replicated heart function of the phantom. Lastly, the phantom must allow for the training of iCMR procedures as this is one of the main goals of the phantom.

3 Design Phase

3.1 Fabrication protocol

For the fabrication of the cardiac phantom, Ecoflex™ 00-10 and 00-50 (Smooth-On, Inc., Macungie, PA, USA) were used. The silicone was prepared using the instructions on the box. To guarantee that the mixture was viscous enough to be poured into the mold, thinner was added. The amount of thinner was determined to be 10% of the volume of the mixture. When all components were added, the mixture was stirred for about three minuted to make sure the it was completely homogeneous. To ensure all air is out of the mixture, the cup was put into a vacuum for a few minutes for degassing. When all bubbles had left the mixture it was ready to be poured using a funnel. The mold was completely filled when the mixture starts coming out of the air holes of the outer mold.

3.2 Cardiac phantom design

For the design of the mold, 3D slicer (3D Slicer 5.6.2, an open-source platform developed by the Slicer Community, Brigham and Women's Hospital, Boston, MA, USA) was used. The 4D XCAT phantom served as a starting point for the model of the blood pool and the myocardium. [21] A few alterations were made to this model, like thinning the walls of the ventricles, to make sure the phantom will simulate the heart properly. In a actual heart, the ventricles have thicker walls to generate the greater force needed for contraction. However, in this model, thinner walls are necessary to achieve greater contraction. Additionally the pulmonary loop was bypassed in this model for simplification.

3.3 Iteration 1

3.3.1 Design

For the first iteration of the mold, the decision was made to create it out of two parts, an inner and an outer mold. This would enable removal of the inner mold later on. For the outer mold a cylinder was created in 3D slicer. From the obtained cylinder, the blood pool and the myocardium were subtracted, after which the cylinder was split to create two hollow halves. Indents were created to make sure the both halves would stay in the right position. The outer mold was printed out of polylactic acid (PLA) using a filament printer (X1E, Bambu lab, Shenzen, China). For the inner mold a segmentation of the blood pool was used. the blood pool was split in half as well to make the printing easier. Two pins were added in the bypass for the pulmonary loop, so that the two pieces of the blood pool can be put together in the correct way. Finally a pin was added to the bottom to make sure the inner mold will stay in the right place during the pouring of the silicone. The two parts of the blood pool were printed out of water soluble polyvinyl alcohol (PVA) using a different filament printer (S7, UltiMaker, Utrecht, the Netherlands). This way the model can be taken out of the outer mold and put into water to dissolve the inner mold, resulting in a hollow phantom. In this iteration Ecoflex™ 00-10 was used and poured according to the fabrication protocol. A visualization of this design can be found in appendix A1 in figure15. Both the inner and outer mold were printed at 50% of the size to test the fabrication procedure

3.3.2 Evaluation

Upon printing both molds, it was immediately evident that there was a design flaw. Due to the way the exterior mold was manufactured, most of the blood pool's volume would be concentrated in one of the halves. Resulting in the entrance of the outer mold being smaller than the inner mold itself. Making it impossible to enter the inner mold as a whole. In addition there was an issue with the way the 2 parts of the blood pool were supposed to connect. Since the model was printed at 50% scale the pins were very small. This resulted in them breaking of. Lastly, the pin added for centering the inner mold was unable to be inserted into the hole in the outer mold, leading to the inner mold not being centered. However, with the use of glue, the molds were still assembled and functional for pouring the silicone. Following the dissolution of the inner mold it was noted that certain flaws were caused by the issue with centering. As seen in figure 4 the silicone was not evenly distributed. Furthermore, the used silicone was very flexible and sticky. Consequently, a different type of silicone was chosen for the further iterations.

Figure 4: Silicone model of iteration 1

3.4 Iteration 2

3.4.1 Design

In the second iteration, 3 support pins were added to center the inner mold elements. There was no margin taken because it was expected that the smallest possible margin would be quite large relative to the size of the pins, which would again result in incorrect centering. After the first iteration it was decided a stiffer silicone would be necessary to simulate the heart properly so this time Ecoflex™ 00-50 was used and poured according to the fabrication protocol. Furthermore the cut of the blood pool was made in a different location, making the assembling easier and more accurate. A visualization of this design can be found in appendix A1 in figure16.

3.4.2 Evaluation

Using no margin on the support pins turned out to be a mistake as they did not fit into the outer mold. Subsequently the beams had to be made smaller manually. Since the 00-50 silicone has a processing time of eighteen minutes rather than the thirty minutes for the 00-10 silicone, the silicone hardened too fast and the mold could not be filled all the way. Due to this it was decided to take the mold apart and put a newly made mixture inside. This mixture was degassed for a shorter amount of time so that the stiffness of the 00-50 silicone could still be evaluated.

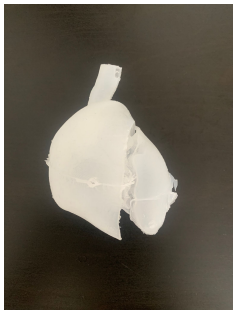

Figure 5: Silicone model of iteration 2

After curing the silicone and removing the outer mold it became clear that the blood pool was not printed out of water soluble PVA. After realising a mistake had been made with the printer, the inner mold was broken and taken

out of the silicone phantom as carefully as possible so that the model could still be used to evaluate the material properties. It was concluded that this type of silicone (00-50) was indeed the better option and it will be used in following iterations.

3.5 Final design

3.5.1 Design

As concluded from iteration 2, in the final design a margin for the support pins was necessary. Furthermore, both the pouring hole and the air holes were positioned differently to optimize pouring. For the pouring hole a spot was chosen where there was adequate room between the inner and the outer mold. The amount of air holes was doubled and they were positioned at the highest point in the outer mold. Additionally, they were made much smaller to avoid an abundance of silicone that would later need to be removed. The blood pool was made smaller with a margin of one millimeter in all directions. This way the cardiac walls of the model will be thicker and able to withhold more pressure during testing. This would help in simulating the heart better. Lastly, the pins created holes in the phantom. These were fixed by breaking of the pins after curing an filling the resulting holes with a newly made mixture of 00-50 silicone.

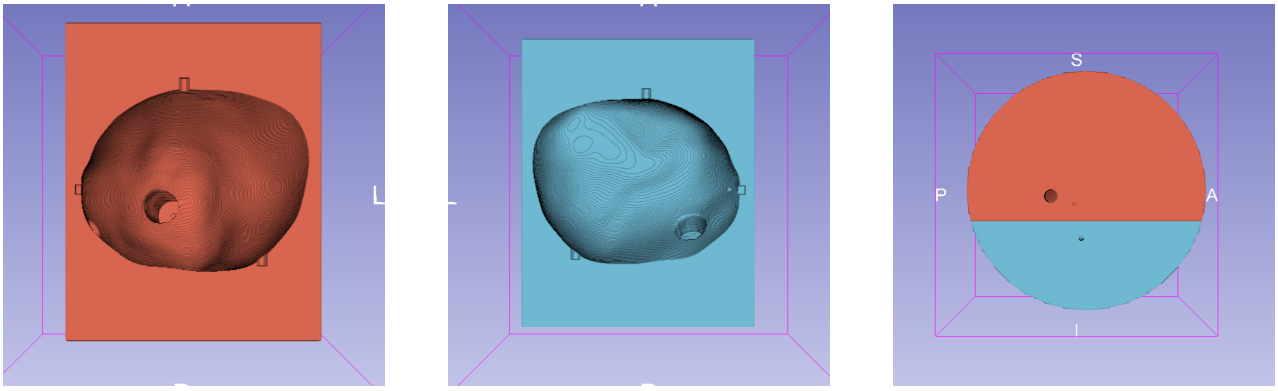

(a) Halve of the outer mold (b) Halve of the outer mold (c) Top of the outer mold including the pouring and air holes

Figure 6: Design of the outer mold in 3D slicer

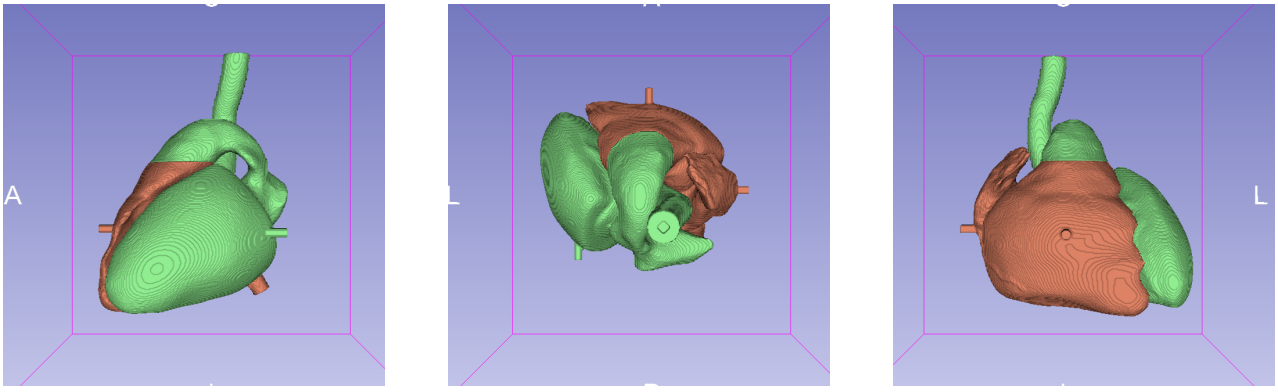

(a) (b) (c)

Figure 7: Design of the complete inner mold, the blood pool, from three different angles in 3D slicer

3.5.2 Evaluation

The final iteration was printed in 100% size. During printing there was a slight error causing the inner mold to be printed incorrectly. As seen in figure 8 this created a hole in the bypass of the pulmonary loop. Even though this part is not critical to simulating the heart, FIMO clay was used to fix the original anatomy. FIMO is a type of clay that does not harden under room temperature and thus will be easily removable along with the blood pool. Other than this printer error, both the inner and outer mold fitted together perfectly. After pouring, curing and removing the mold a suitable, leakage free cardiac phantom was created as seen in figure 10.

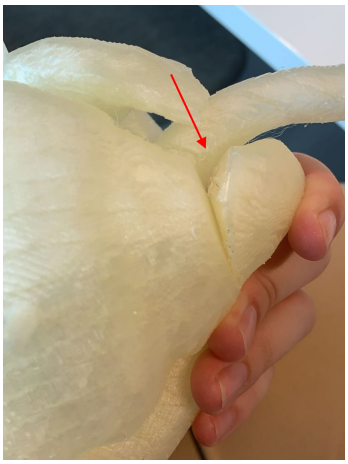

Figure 8: Printing error in the blood pool

Figure 9: Solution to printing error with FIMO clay

Figure 10: Final cardiac phantom

4 Validation phase

4.1 Methods

4.1.1 Function

To asses whether the phantom is indeed dynamic per requirement *2.1: The phantom is dynamic*, testing was conducted using a pressure vessel. For this pressure vessel a cylinder made out of perspex was used as seen in figure 11a. The vessel was filled with water and connected to the Vivitro superpump AR series (Vivitro Labs Inc., Victoria, BC, Canada). Subsequently the phantom was filled with water, connectet to tubes that were also filled with water, and placed within this vessel. Pressure was then added to the vessel using the pump to create contraction and relaxation in the phantom by external pressure. A dynamic image will be acquired using MRI techniques to demonstrate change in volume. Requirement *2.2: The phantom stays intact at normal heart pressure* will be tested as well by turning the pump to this pressure and observe the structural integrity of the phantom. Finally, to review requirement *2.4: The phantom allows for the training of iCMR procedures* testing will be done to see if the phantom is appropriate for training iCMR techniques such as catheter ablation. For these tests a catheter was inserted into the phantom and tracked using MRI. Figure 11a shows the materials needed to create the setup seen in Figure 11b. To maintain the phantom in the center of the vessel, a 3D printed halve cylinder equipped with rope was designed in SOLIDWORKS 2024 (SOLIDWORKS, Dassault Systèmes, Waltham, MA, USA). Valves were added to the tubes connected to the aorta and the vena cava to ensure one way flow towards and from the water reservoir. Furthermore a component enabling the insertion of a catheter, indicated with the red arrow, was added. An additional component of this set up was a long water-filled tube that was connected at the location of the blue arrow seen in figure 11b. The pump and vessel were linked by this tube.

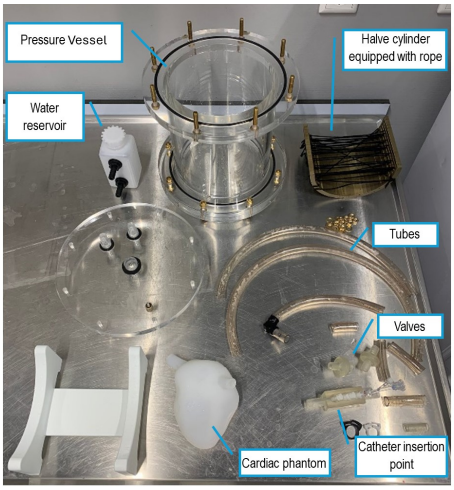

(a) Materials needed to achieve the set up visible in b).

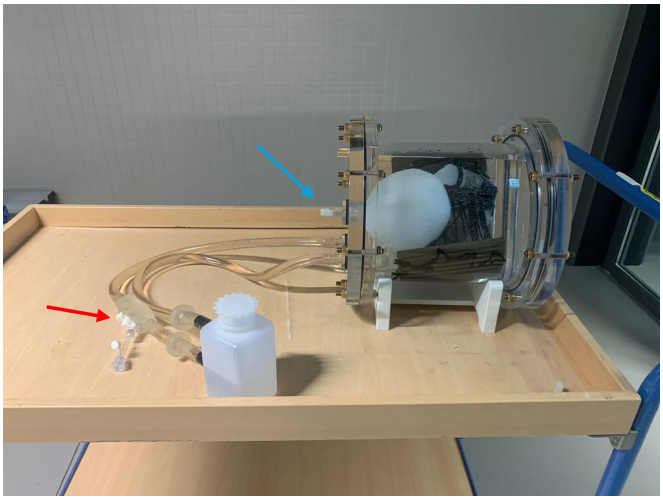

(b) Set up for both the pressure test and the test in the MRI. The blue arrow indicates the connecting point of the pump and the red arrow indicates the insertion point of a possible catheter.

Figure 11: a) Materials needed for the set up. b) Set up for testing

The entire set up was subsequently put into a MRI. The testing was performed on a Siemens 1.5 T MRI (Aera, Siemens Healthineers, Erlangen, Germany). The long tube connecting the set up to the pump was pulled through the wall of the MRI room so that the pump could be stationed outside of this room. The gain was gradually increased and ultimately set to 50,6% based on visual inspection. The MRI system was synchronized with the pump using a signal generator which was triggered by the pump.

4.1.2 Pressure curves

In accordance with requirement *2.3: The phantom allows for pressure curves to be created*, tests were done to measure the pressure in one of the ventricles. The pressure was measured and compared to physiological values and used to validate whether the cardiac phantom properly simulates an actual heart. In order to measure this pressure, a catheter is inserted into the right ventricle through the vena cava. The same set up as presented in section 4.1.1 was used. The catheter was inserted at the position indicated with the red arrow.

Pressure measurements were recorded using a Swan-ganz catheter coupled to a APT300 pressure sensor with a range of up to 250 mmHg and a custom labview script. The obtained data was converted using MATLAB (R2023b, Mathworks, Natick, MA, USA) to the pressure curves seen in figure 14a and 14b

4.1.3 Remaining requirements

To verify compliance, the factual requirements 1.1, 1.2, 1.3, 1.4, 1.5 and 1.6 were evaluated using a PASS/FAIL system.

4.2 Results

4.2.1 Function

In the dynamic image it is evident that the phantom contracts, albeit minimally. Figures 12a and 12b display two snapshots from this video corresponding to diastole (figure 12a) and systole (figure 12b). A measurement taken at the same location shows a slight variation in width of roughly six millimeters. Figures 13a and 13b depict the catheter being inserted into the phantom from various perspectives.

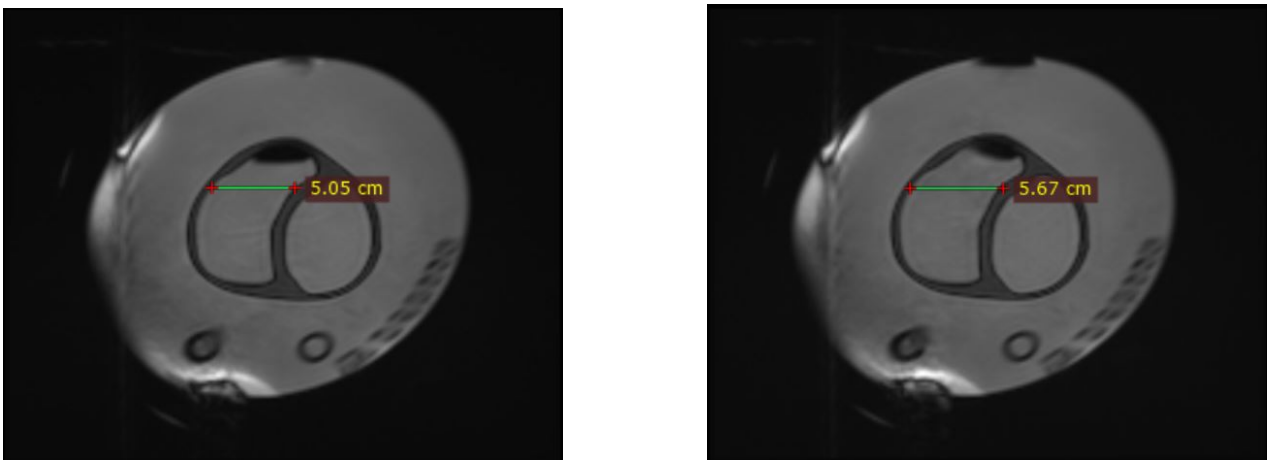

(a) (b)

Figure 12: Two snapshots of the dynamic image showing contraction of the phantom. Figure a) showing diastole and figure b) showing systole

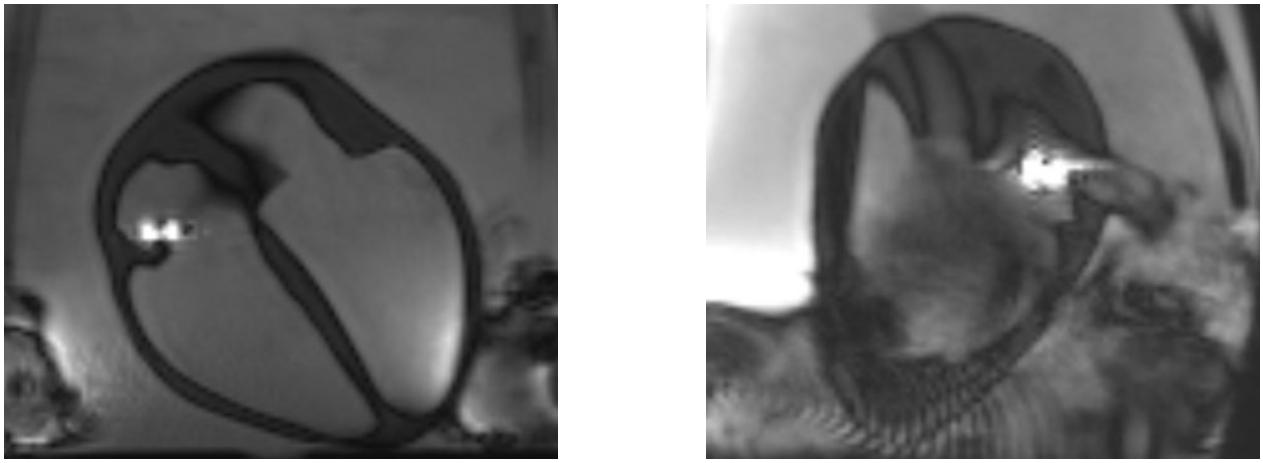

(a) (b)

Figure 13: Insertion of the catheter shown in two different perspectives

4.2.2 Pressure curves

Figures 14a and 14b show the measured pressure curves with two different settings on the pump. When the pump was set to 13,4% gain, the pressure in the right ventricle was on average 155 mmHg, with a systolic pressure of about 230 mmHg and a diastolic pressure of about 95 mmHg When the pump was set to 7% gain, the pressure was on average 145 mmHg, with a systolic pressure of about 180 mmHg and a diastolic pressure of about 115 mmHg. It was noted that the phantom stayed intact during these measurements.

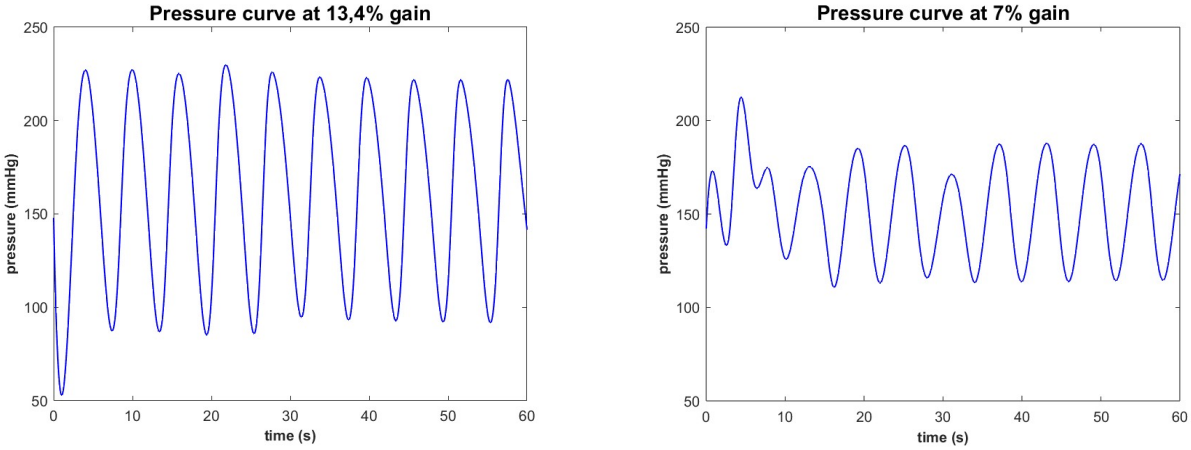

(a) Pressure curve at 13,4% gain

(b) Pressure curve at 7% gain

Figure 14: Pressure curves measured in the right ventricle using the Vivitro superpump AR series

4.2.3 Remaining requirements

A PASS was assigned to four out of six requirements. Two requirements were labelled with a FAIL. The Youngs modulus of Ecoflex™ 00-50 is about 82 kPa whereas the Youngs modulus of myocardial tissue is below 50 kPa. [22] [23]. Furthermore the phantom does not contain any valves.

Table 2: PASS/FAIL requirements

1.1	The phantom is made out of silicone	PASS
1.2	The phantom has a Youngs modulus comparable to the myocard	FAIL
1.3	The atria and ventricles of the phantom are anatomically correct	PASS
1.4	The phantom is MR compatible	PASS
1.5	The blood pool is not included in the phantom	PASS
1.6	The phantom contains valves	FAIL

5 Discussion

During this thesis the main aim was the development of a dynamic cardiac phantom for the purpose of training and advancing minimally invasive iCMR procedures. The chosen approach was to use silicone for the fabrication and to validate the obtained phantom by creating pressure curves and dynamic imaging using MRI techniques.

5.1 Theoretical discussion

The contraction of the phantom was, though minimal, present. This confirms requirement *2.1: The phantom is dynamic.* The limited contraction could be explained by the fact that the phantom is quite large in comparison to a human heart. An average human heart is about 12 centimeters in height and 9 centimeters in width. [24] The phantom is about 15 centimeters in height and 11 centimeters in width. It was believed this size difference would not have a big influence since the proportions are equal. However, the power of the pump was not taken into account. The pump must deliver more power if the phantom is bigger, so this could have influenced the size of contraction.

In figure 13, insertion of the catheter into the right atrium is shown. These images, made using MRI, confirm that the phantom meets requirement *2.4 The phantom allows for the training of iCMR procedures* since it is possible to real-time see, and track a catheter in this phantom.

The pressure curves in figure 14 show relatively high values. Both settings show an average of about 150 mmHg, with peak pressures up to 230 mmHg. The average peak ventricular pressure is 120-150 mmHg. [20] However, since these values are higher than those of a regular heart, requirement *2.2 The phantom stays intact at normal heart pressure* is passed, as the phantom stayed intact at higher pressure. Furthermore, during the testing in the MRI the pump was set to 50,6% gain indicating that the phantom can withstand much higher pressures. The acquired pressure curves confirm requirement *2.3: The phantom allows for pressure curves to be created.* The only drawback was that the pressure could not be measured in the MRI room. If this had been possible and if the required software had been available, tests could have been conducted to determine whether the phantom is suitable for validating heart function.

Lastly, requirement *1.2: The phantom has a Young's modulus comparable to the myocard* was labeled as a FAIL. However, this does not necessarily compromise the phantom's functionality. The Young's modulus measures the elasticity of the material. Since the phantom is designed to contract due to external pressure rather than stretch, the difference in Young's modulus does not affect the suitability of the silicone for this application.

5.2 Technical discussion

Several things did not go as expected during the phantom's design and fabrication. First of all, the inner mold from the first iteration was printed out of water soluble PVA. However, the support material was printed using the same water soluble PVA. Because of this, the support material merged with the

actual model making it very difficult to extinguish and remove it. This resulted in an inner mold that was not anatomically correct. Furthermore, during the second iteration the inner mold was printed out of a different material than the water soluble PVA due to miscommunication at the printer. It is possible that the coils were switched, resulting in a inner mold that did not dissolve. The phantom had to be cut open to take the inner mold out. Due to this, it was not possible to properly asses the 00-50 silicone.

During the first pouring of the 00-50 silicone, the setting time was not taken into account. The 00-50 silicone started curing in just eighteen minutes. This resulted in an already low viscosity after degassing, making it impossible to pour into the mold. In the third iteration this curing time was taken into account. However, this limited the degassing time to about six minutes. This could possibly have resulted in air bubbles still being present in the phantom. Yet, visually looking at the phantom, no air bubbles were to be seen. Because of the fast curing time, the 100% model had to be poured in three different phases. This could have caused contamination between the layers.

Finally, the vena cava wall tore just before testing. It is probable that the inner mold was not put together properly after breaking in multiple places, resulting in incorrect centering. This caused the vena cava to be much thinner in one area which is also where it tore. By using additional silicone in this area, the rip was able to be repaired. A lot of force was applied to this vein when inserting the phantom into the pressure vessel. In order to make sure both the vein and the artery can withstand this force, thickening of both of these walls is preferred.

5.3 Future recommendations

Further research is necessary to perfect the cardiac phantom. First of all the phantom is currently not completely anatomically correct since there were no valves involved. Adding valves would make the phantom a more reliable representation of the heart. Inspiration for how to add these valves can be taken from Laing et al. [15] Their phantom, though not anatomically correct, did involve valves. In addition it would be interesting to use patient data for the design of the blood pool and the myocard. For this research, the 4D XCAT phantom was used as a starting point.[21] However, by using actual patient data it would be possible to create a patient-specific cardiac phantom that could be used to practice procedures that would be carried out on said patient. This would enhance the operational planning process. Furthermore, to determine whether the phantom can be used for validating heart function, it is essential to generate pressure-volume loops. However, in this research, the necessary tools and software required for creating these loops were not available. Therefore it is recommended that these tests will be performed in future research. Lastly, further research in the potential silicone's is required. The limited amount of possibilities in this research may have prevented a perfect match.

6 Conclusion

A dynamic cardiac phantom has been designed and validated in this paper. Upon reexamining the research question: *"What is the feasibility of using silicone to create a dynamic cardiac phantom that would be used for the training and development of iCMR procedures?"* it can be concluded that silicone is a suitable material for this application. The phantom has to be refined and developed further, but overall, this research has produced a phantom that is suitable for use in training and improving iCMR techniques.

References

[1] Who WHO. Cardiovascular diseases. World Health Organization: WHO. 2019 Jun. Available from: https://www.who.int/health-topics/cardiovascular-diseasestab=tab$_1$.

[2] Ziekten van hart en vaatstelsel | Sterftecijfers | Volksgezondheid en Zorg; 2024. [Online; accessed 5. May 2024]. Available from: https://www.vzinfo.nl/hart-en-vaatziekten/sterftecijfers.

[3] Rogers T, Lederman RJ. Interventional CMR: Clinical Applications and Future Directions. Curr Cardiol Rep. 2015 May;17(5):1-9. doi:10.1007/s11886-015-0580-1.

[4] Lederman RJ. Cardiovascular Interventional MRI. Circulation. 2005 Nov;112(19):3009. doi:10.1161/CIRCULATIONAHA.104.531368.

[5] Rogers T, Campbell-Washburn AE, Ramasawmy R, Yildirim DK, Bruce CG, Grant LP, et al. Interventional cardiovascular magnetic resonance: state-of-the-art. J Cardiovasc Magn Reson. 2023 Feb;25(1):48. doi:10.1186/s12968-023-00956-7.

[6] de A Brandão CM, Dallan LRP, Dinato FJ, Monteiro R, Fiorelli AI, Jatene FB. Evaluation method of training simulation on biological models for cardiovascular surgery residents. J Card Surg. 2021 Jul;36(7):2247-52. doi:10.1111/jocs.15524.

[7] What the Heart Looks Like; 2024. [Online; accessed 5. May 2024]. Available from: https://www.nhlbi.nih.gov/health/heart/anatomy.

[8] Kuehne T, Yilmaz S, Steendijk P, Moore P, Groenink M, Saaed M, et al. Magnetic Resonance Imaging Analysis of Right Ventricular Pressure-Volume Loops. Circulation. 2004 Oct. Available from: https://www.ahajournals.org/doi/full/10.1161/01.CIR.0000143138.02493.DD.

[9] Pressure-Volume Loop Relationships | EDPVR and ESPVR | ADInstruments; 2024. [Online; accessed 6. May 2024]. Available from: https://www.adinstruments.com/blog/introduction-pv-loops-understanding-points-pv-loop-and-measures-cardiac-function.

[10] Bowen DL, Touchet TJ, Maitland DJ, McDougall MP. Technical note: The design and validation of a multi-modality lung phantom. Med Phys. 2023 Aug;50(8):4809-15. doi:10.1002/mp.16462.

[11] Kashif AS, Lotz TF, McGarry MD, Pattison AJ, Chase JG. Silicone breast phantoms for elastographic imaging evaluation. Med Phys. 2013 Jun;40(6Part1):063503. doi:10.1118/1.4805096.

[12] Lamouche G, Kennedy BF, Kennedy KM, Bisaillon CE, Curatolo A, Campbell G, et al. Review of tissue simulating phantoms with controllable optical, mechanical and structural properties for use in optical coherence tomography. Biomed Opt Express. 2012 Jun;3(6):1381. doi:10.1364/BOE.3.001381.

[13] Guimarães CF, Gasperini L, Marques AP, Reis RL. The stiffness of living tissues and its implications for tissue engineering. Nat Rev Mater. 2020 May;5:351-70. doi:10.1038/s41578-019-0169-1.

[14] Sindi R, Wong YH, Yeong CH, Sun Z. Development of patient-specific 3D-printed breast phantom using silicone and peanut oils for magnetic resonance imaging. Quantitative Imaging in Medicine and Surgery. 2020 Jun;10(6):1237. doi:10.21037/qims-20-251.

[15] Laing J, Moore JT, Vassallo R, Bainbridge D, Drangova M, Peters TM. Patient-specific cardiac phantom for clinical training and preprocedure surgical planning. Journal of Medical Imaging. 2018;5(2):021222. Available from: https://doi.org/10.1117/1.JMI.5.2.021222. doi:10.1117/1.JMI.5.2.021222.

[16] Kolawole FO, Peirlinck M, Cork TE, Levenston M, Kuhl E, Ennis DB. Validating MRI-Derived Myocardial Stiffness Estimates Using In Vitro Synthetic Heart Models. Ann Biomed Eng. 2023 Jul;51(7):1574-87. doi:10.1007/s10439-023-03164-7.

[17] Bietenbeck M, Florian A, Chatzantonis G, Meier C, Korthals D, Martens S, et al. Introduction of a CMR-conditional cardiac phantom simulating cardiac anatomy and function and enabling training of interventional CMR procedures. Scientific Reports. 2019 12;9. doi:10.1038/s41598-019-56506-8.

[18] Cohrs NH, Petrou A, Loepfe M, Yliruka M, Schumacher CM, Kohll AX, et al. A Soft Total Artificial Heart—First Concept Evaluation on a Hybrid Mock Circulation. Artif Organs. 2017 Oct;41(10):948-58. doi:10.1111/aor.12956.

[19] Miranda E. MoSCoW Rules: A quantitative exposé (Accepted for presentation at XP2022). 2021 12.

[20] Kono A, Maughan WL, Sunagawa K, Hamilton K, Sagawa K, Weisfeldt ML. The use of left ventricular end-ejection pressure and peak pressure in the estimation of the end-systolic pressure-volume relationship. Circulation. 1984 Dec. doi:10.1161/01.CIR.70.6.1057.

[21] Segars WP, Sturgeon G, Mendonca S, Grimes J, Tsui BMW. 4D XCAT phantom for multimodality imaging research. Med Phys. 2010 Sep;37(9):4902. doi:10.1118/1.3480985.

[22] Allijn I, Ribeiro M, Poot A, Passier R, Stamatialis D. Membranes for Modelling Cardiac Tissue Stiffness In Vitro Based on Poly(trimethylene carbonate) and Poly(ethylene glycol) Polymers. Membranes. 2020 Oct;10(10):274. doi:10.3390/membranes10100274.

[23] ; 2024. [Online; accessed 19. Jun. 2024]. Available from: https://www.smooth-on.com/tb/files/ECOFLEX$_S ERIES_T B.pdf$.

[24] Mohammadi S, Hedjazi A, Sajjadian M, Ghoroubi N, Mohammadi M, Erfani S. Study of the normal heart size in Northwest part of Iranian population: a cadaveric study. Journal of Cardiovascular and Thoracic Research. 2016;8(3):119. doi:10.15171/jcvtr.2016.25.

Appendix

A1 Design process

Iteration 1

The figures below illustrate the design of the outer and inner molds of iteration 1. Figures 15a to 15c show the outer mold, where the two halves with the indents and the two pouring holes are visible. Figures 15d to 15f show the inner mold, clearly displaying the two pins connecting the halves and the additional support pin for the centering of the inner mold.

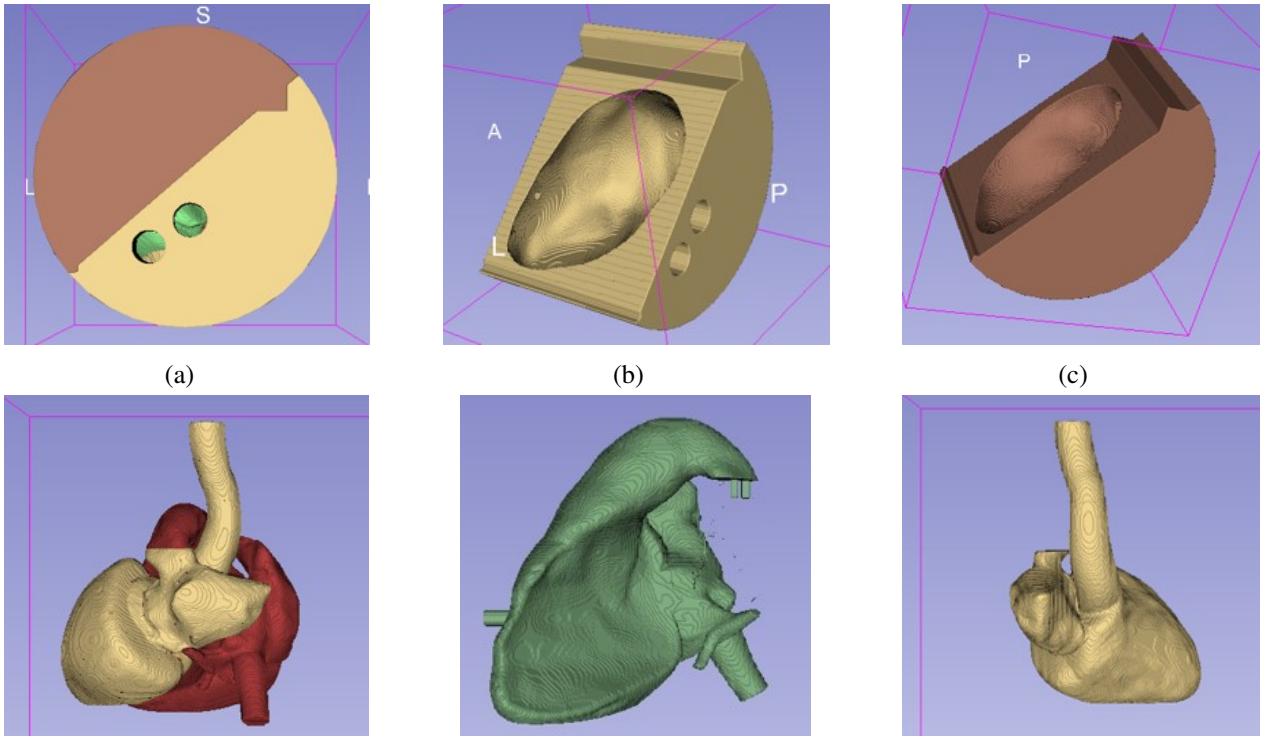

(a) (b) (c)

(d) (e) (f)

Figure 15: Iteration 1, a), b) and c) show the outer mold from different perspectives and d), e) and f) show the inner mold from different perspectives

Iteration 2

The figures below illustrate the design of the outer and inner molds of iteration 2. Figures 15a to 15c show the outer mold, where the different split, resulting in a bigger and a smaller halve, and the indents for the support pins are visible. Figures 15d to 15f show the inner mold, displaying the three support pins as well as the indent in the aorta and the two pins connecting the halves. Furthermore it is seen that the three support pins are wider than those in the final design and that the inner mold was split in halve at a different location than in iteration 1.

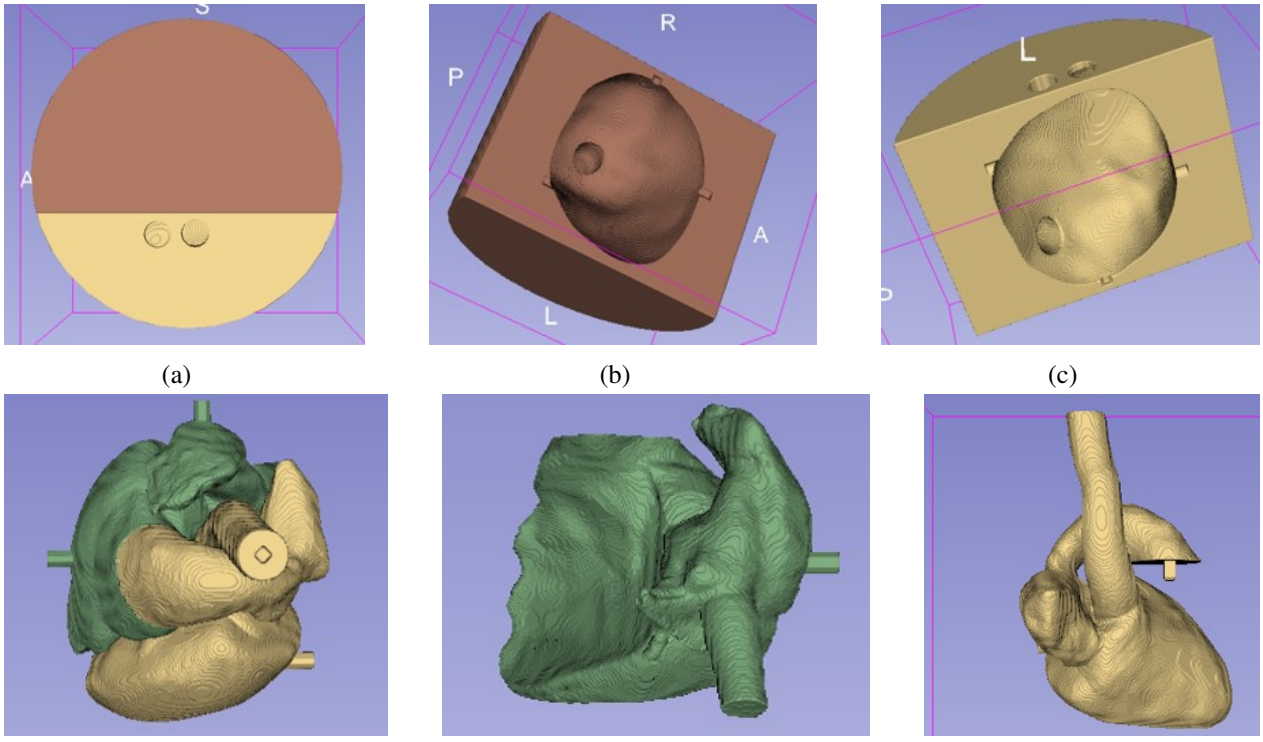

(a) (b) (c)

(d) (e) (f)

Figure 16: Iteration 2, a), b) and c) show the outer mold from different perspectives and d), e) and f) show the inner mold from different perspectives

List of Tables

List of Figures